The passivation of electrically active sites on the surface of crystalline silicon by fluorination

B. R. Weinberger, H. W. Deckman, E. Yablonovitch, T. Gmitter, W. Kobasz, and S. Garoff
Corporate Research Laboratory, Exxon Research and Engineering Company, Annandale, New Jersey 08801

(Received 19 October 1984; accepted 27 December 1984)

A nonoxide surface passivation for crystalline silicon is described. It involves the fluorination of the silicon surface. Characterization by photoconductive lifetime measurements and *C–V* measurements on MIS structures indicate that the fluorinated silicon surface is extraordinarily electrically passive, $\lesssim 10^{10}$ traps per cm^2. Our technique for producing such high quality surfaces is described as is a novel gate insulator structure employing organic thin films. Potential device advantages of this alternative to oxide technology are also discussed.

I. INTRODUCTION

It is well known that the termination of the ordered crystalline lattice at the surface of a semiconductor results in a surface electronic configuration drastically different from that found within the bulk of the semiconductor. Situations such as distorted bonds or unsatisfied dangling bonds at the surface create electronic states within the semiconductor's forbidden energy gap. Such states which may trap and immobilize charge or randomly generate mobile charge thermally are parasitic to the proper operation of semiconductor devices, particularly surface junction devices like MISFET's. A crucial property of crystalline silicon which to a great measure has been responsible for its technological importance is the high quality of the interface it can form with its oxide. Thermally oxidized and annealed silicon surfaces can exhibit nearly perfect passivation, midgap densities of states as low as 1×10^{10} states /eV cm^2 or ~ 1 surface state per 10^5 surface atoms.[1]

While Si–SiO_2 interfaces produce a low surface state density near the center of the silicon band gap, the density of states may increase rapidly toward the band edges in a characteristic U-shaped distribution.[2] This may lead to excessive recombination losses in Si solar cells which require the use of heavily doped highly conducting Si with Fermi levels near the band edges to minimize series resistance effects. Further, while the Si–SiO_2 interface may produce a minimal density of states within the gap, the amorphous SiO_2 may contain a high density of defect states. These states may be charged, causing alteration of MOSFET threshhold voltages, or uncharged but a tunnellable distance from the interface so that hot electrons from the device channel may be trapped. The latter effect will be particularly pronounced in short channel devices because of the large electric fields present. SiO_2 is also susceptible to degradation by exposure to radiation via photoinduced occupation of previously neutral trap sites or bond disruption creating new traps. The mitigation of such radiation sensitivity in MOS devices is important in military and space applications.

Therefore, despite the great technological success of the oxide passivated crystalline silicon surface, alternate forms of lattice terminations for silicon are of more than academic interest. Early on, before silicon–oxide technology was firmly established, so-called "real" chemically treated and etched silicon surfaces were studied.[3] Some success in surface passivation was achieved. However, none achieved the stability in ambient atmospheres required for device fabrication. Recently, the use of epitaxial insulators such as CaF_2 has been explored as potential low defect heterolayers on silicon.[4–7] Alternate insulators such as Langmuir–Blodgett organic films deposited on top of a thin silicon native oxide layer have also been studied.[8,9] To date, these alternate surface passivations have not achieved the quality of the Si–SiO_2 interface.

In this paper, we describe a nonoxide silicon surface termination which produces an interface of extraordinary electronic quality. We have found that a silicon surface terminated with fluorine bonds is nearly free of any surface electronic states within the silicon energy gap. We have measured, using a photoconductive decay technique, surface recombination velocities as low as 4 cm/s for the fluorine terminated silicon surface. Midgap interface state densities as low as 3×10^9/eV cm^2 have been measured on MIS structures with fluorinated surfaces using standard capacitance–voltage (CV) measurements with nonlattice matched polycrystalline insulators. Measurements of surface recombination velocity performed on surface fluorinated silicon wafers appear to be weakly dependent on bulk doping levels suggesting that, unlike oxidized surfaces, the surface state density on fluorinated wafers does not rise precipitously away from midgap. Our results suggest that a silicon interface technology based on fluorine chemistry may for many applications be superior to that based on oxide chemistry.

II. WAFER PREPARATION

Silicon wafers employed in this study were high bulk quality (bulk minority carrier lifetime $\tau_B \geqslant 3$ ms) float zone material obtained from Wacker Chemitronics. This high bulk quality enhanced the surface sensitivity of our characterization probes. *n*- and *p*-type wafers both (100) and (111) crystallographic orientation were studied.

Several silicon surface chemical treatments were employed with varying degrees of success at passivation. These are listed in Table I. Of note is that technique 4 yielded poorly passivated surfaces despite the similarity to the highly successful technique 1. Preliminary XPS data suggest that

 0734-2101/85/030887-05$01.00

TABLE I. Silicon surface treatments.

	Step 1	Step 2	Surface recombination velocity achieved
1	CP-4 etch	HF acid dip	4 cm/s
2	Thermal oxidation	HF acid dip	4 cm/s
3	HF acid oxide removal	XeF_2 vapor	40 cm/s
4	KOH etch	HF acid dip	> 300 cm/s

the techniques employing a final hydrofluoric acid immersion step produce a silicon surface terminated with fluorine bonds similar to that obtained by procedure 3.[10]

The apparatus we have assembled for wafer processing is displayed in Fig. 1. The data presented in this paper are for wafers prepared using techniques 1 and 2. The silicon wafer is mounted in a stainless steel cross on a Teflon rod. The rod passes through an O-ring compression seal which permits both rotary and linear manipulation of the wafer. We have found that exposure of a fluorinated wafer to air results in a rapid deterioration of the surface passivation. The apparatus in Fig. 1 permits all operations (etching, fluorination, subsequent coating depositions) to be performed either in an inert Ar atmosphere or under vacuum.

Oxide removal and fluorination of the wafer surface is accomplished by first purging the system with Ar, then immersing the wafer in an aqueous HF solution contained in a Teflon vessel suspended below the cross and separated from it by a gate valve. The fluorinated wafer may then be withdrawn back into the cross without exposing the surface to air. Air impermeable coatings are applied to the passivated surfaces by evacuating the cross through a second gate valve and depositing material from thermal evaporation sources through this same valve.

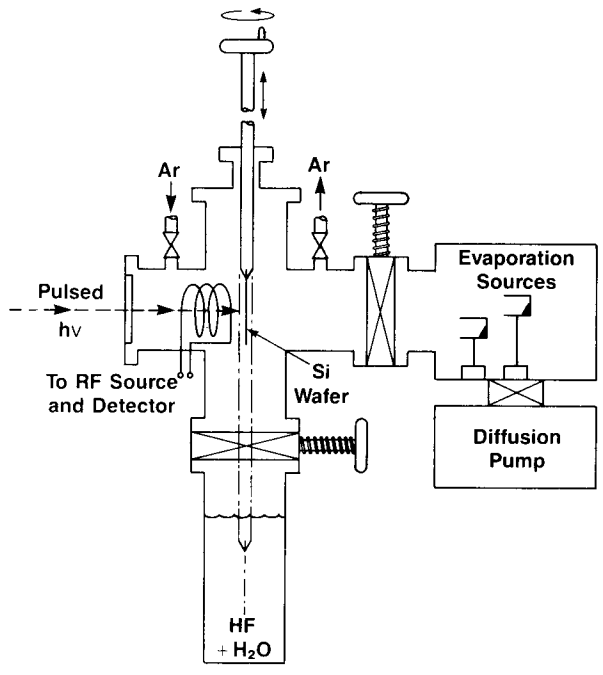

FIG. 1. Wafer processing apparatus used in this work.

III. PHOTOCONDUCTIVE LIFETIME MEASUREMENTS

Also included in the cross is an rf coil *inductively* coupled to the silicon wafer. A transparent window is placed on one arm of the cross allowing illumination of the wafer. The condition of the wafer surface is monitored *in situ* via the transient photoinduced eddy current losses following pulsed illumination of the wafer. From this photoconductive decay the minority carrier lifetime may be determined and the surface recombination velocity inferred.[11] Because of the geometry portrayed in Fig. 1, the surface passivation may be monitored *during* the evaporative coating process. The transient photoconductive decay technique is particularly suited to the study of well passivated silicon surfaces important in device technology. The surface sensitivity is limited only by the bulk quality of the material. In the work presented here, we have been able to detect electrically active surface states at a level of $1/10^6$ surface atoms, a sensitivity far exceeding that of other surface analytical tools.

The photoconductivity decay rate will be sensitive to surface recombination for thin wafers of high quality (long τ_B). The excess minority carrier density (holes for a n-type wafer) will be governed by a one dimensional diffusion equation:

$$D_p \frac{d^2p}{dx^2} - \frac{p-p_o}{\tau_B} = \frac{dp}{dt}. \tag{1}$$

The second term describes bulk recombination and the first term governs diffusion to the surface which when coupled with the boundary condition:

$$D_p \frac{dp}{dx} = p S_p, \quad x = O,L \tag{2}$$

includes the effect of surface recombination where D_p and S_p are the diffusion constant and surface recombination velocity for holes and L is the thickness of the wafer. In the absence of surface charging, S_p is time independent and the solution to Eq. (1) will have a time dependence of the form:

$$p(x,t) \propto \exp -\left(\frac{1}{\tau_B} + \frac{1}{\tau_S}\right) t = \exp -\left(\frac{t}{\tau_{\rm ph}}\right), \tag{3}$$

where τ_s is the surface recombination lifetime and $\tau_{\rm ph}$ is the measured photoconductive lifetime.

For well-passivated surfaces where $S \ll D_p/L$

$$1/\tau_s = 2S_p/L. \tag{4}$$

A representative photoconductive decay curve is shown in Fig. 2. The data were obtained for a fluorine passivated (100) n-type wafer ($L = 275\ \mu$, dopant density $N_D = 10^{15}/\text{cm}^3$) with the coating layers shown in the inset. The measured $\tau_{\rm ph}$ of 550 μs implies a surface recombination velocity $S_p \leqslant 25$ cm/s. The upper bound assumes an infinite τ_B. If one assumes equal electron and hole capture cross sections and low level injection, for a density of surface states N_s at midgap[12]:

$$S_p = N_s\, v_t\, \sigma, \tag{5}$$

where v_t is the thermal velocity for electrons, 10^7 cm/s.

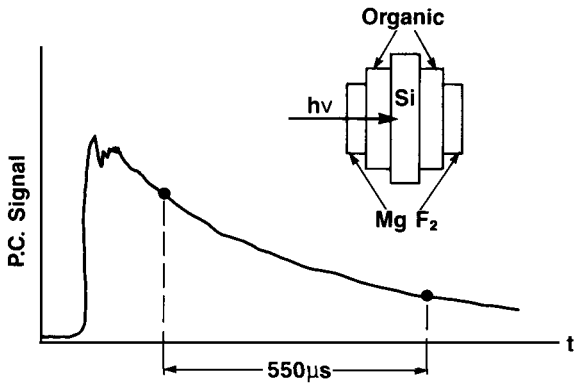

FIG. 2. Photoconductive decay obtained for fluorinated silicon wafer (n-type, 5Ω-cm, $L = 275\ \mu$) coated with composite insulator, as measured in air.

Typical values for surface state hole capture cross sections obtained for oxidized surfaces are $\sigma \sim 5\times10^{-16}$ cm^2.[13] The measured τ_{ph} therefore implies a midgap surface state density of $<5\times10^9$ cm^{-2}, or less than one electrically active interface trap per 10^5 surface atoms.

Measurements of τ_{ph} as large as 3 ms on fluorinated 275 μ thick wafers have been routinely obtained. Implied is a surface recombination velocity, assuming only surface recombination and no bulk recombination, $S_p \leqslant 4$ cm/s. Such results are independent of the crystallographic orientation of the wafer, (100) or (111). Significantly, such long surface photoconductive lifetimes have been obtained by fluorinating surfaces of wafers with widely varying conductivities. Surface recombination velocities less than 12 cm/s have been measured on n-type fluorinated wafers with dopant densities varying over the range $5\times10^{13} - 1\times10^{17}$ cm^{-3}. In other words, S_p was found to be independent of the position of the majority carrier Fermi level over the range $0.14 < E_C - E_F < 0.33$ eV. The Shockley–Read–Hall treatment of surface recombination[14] demonstrates that under low level carrier injection, those surface states close to the band edges will have little effect on the surface recombination velocity since the residence time of carriers in these traps is too short to permit efficient recombination. In fact, for an n-type semiconductor it may be shown that only those traps with energy E_t in the range $E_v + (E_c - E_F) < E_t < E_F$ are effective. What this implies is that the surface photoconductive lifetime in more heavily doped wafers should be sensitive to surface states nearer the band edges. For thermally oxidized heavily doped wafers, we have been unable to obtain long lifetimes. We take this as a manifestation of the U-shaped density of surface states distribution of the Si–SiO_2 interface where the density of states rises precipitously away from midgap.[2] In contrast, the low S_p measured on fluorinated surfaces of similar wafers with E_f as close as 0.14 eV to the band edge, we take as preliminary evidence that the distribution of surface states associated with the fluorinated surfaces does not have the broad "band tails" the oxidized surface does.

The foregoing analysis is valid for the flat band situation for which surface charging is absent. Consider the case of an n-type wafer with a positive surface charge creating a surface potential of ψ_s placing the surface layer into accumulation. In low level injection Eq. (5) becomes[15]

$$S_p = \sigma V_{th} N_s \exp - (e\psi_s/kT). \quad (6)$$

The recombination velocity in accumulation is *reduced* by the exponential factor. The apparent S_p is diminished without a reduction in surface state density N_s. In effect, the positive surface potential acts as a minority carrier mirror repelling holes from the surface, reducing surface recombination because the arrival rate of minority carriers at recombination centers is the rate determining step in surface recombination. The effects of surface charging may be eliminated by high level injection of carriers which tends to flatten the surface band bending. The presence of appreciable surface charging will be quite apparent in the photoconductive lifetime measurements. The points along the decay, in fact, represent different levels of carrier injection. A strongly nonexponential decay indicates a surface recombination velocity which varies with injection level, or in other words a charged surface. The photoconductive decay displayed in Fig. 2 exhibited no such serious charging effects so that the long photoconductive lifetime is indeed a firm indication of the low density of surface states at the fluorinated surface.

IV. MIS CAPACITANCE MEASUREMENTS

Interface states store electronic charge. Therefore, the density and properties of such states may be probed by studying the capacitance of metal–insulator–semiconductor (MIS) structures as a function of bias voltage and frequency. Several requirements, however, had to be satisfied by the gate electrode for our purposes. The finished device must have an air impermeable encapsulation as air exposure rapidly deteriorates the fluorinated silicon surface. The insulator preferably should only weakly interact with the surface so as not to perturb its near ideal electronic structure. The insulator should have high resistivity and a low density of trapped charge for optimal performance of the MIS device. The insulator should be transparent so that the photoconductive lifetime could be monitored subsequent to and during the deposition. Finally, the insulator should form pinhole free films on room temperature substrates by thermal evaporation so as to be compatible with our apparatus (Fig. 1).

An MIS structure which satisfies the foregoing criteria is shown in the insets to Figs. 2 and 3. The gate insulator employed is a two-layer structure consisting of 1000 Å of a polynuclear aromatic (PNA) organic film capped with 500 Å of MgF_2. The PNA used to obtain the data in Figs. 2–4 was rubrene (5, 6, 11, 12 tetraphenyl-napthacene). It forms high quality pinhole free films from thermal evaporation sources at $\sim$300 °C onto room temperature substrates. Like other PNA's rubrene is a high resistivity insulator.[16] The PNA's form molecular solids with a weak van der Waals intermolecular interaction. Presumably the binding of the rubrene film to the fluorinated silicon surface is of a similar nature. This is consistent with our observation that the deposition has little effect on the measured τ_{ph} (Fig. 2). The PNA's, such as rubrene, however, were found to form only poor

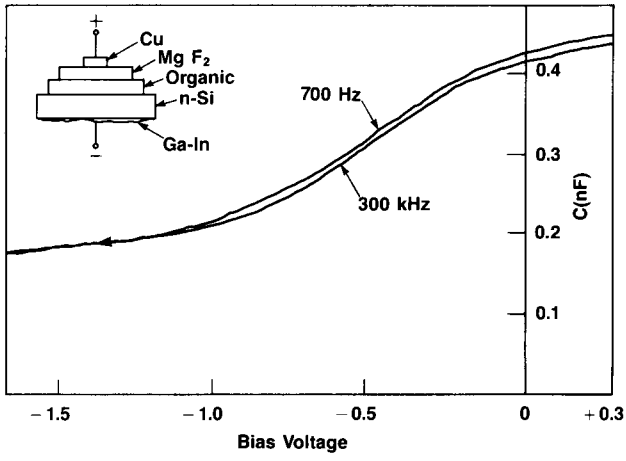

FIG. 3. High and low frequency CV data fluorinated silicon MIS device. (Same wafer as Fig. 2.)

diffusion barriers to air so that long term stability of the MIS devices necessitated an air impermeable overlayer. We found that a 500 Å layer of evaporated MgF_2 served this purpose well. It should be noted that MgF_2 *without* the organic layer present was unsatisfactory as a gate insulator, severe degradation of τ_{ph} being observed during the deposition process. The nature of the interaction between the MgF_2 and the fluorinated silicon surface is uncertain.

Shown in Fig. 3 are high and low frequency capacitance data for the same fluorinated silicon wafer (n-type, 5 Ω-cm) whose photoconductive decay is shown in Fig. 2. The area of the metallic gate electrode was 0.02 cm^2. The capacitance at positive bias (accumulation) should just be a measure of the insulator (C_{ins}) capacitance. We attribute the dispersion between high and low frequency capacitance observed in this bias range to the previously reported frequency-dependent dielectric constant of polycrystalline films of MgF_2.[17] For negative biases (depletion) some of the dispersion between low and high frequency data may be attributed to the long response time of the surface state density D_s and hence the surface state capacitance C_s is given by[18]:

$$e D_s = C_s = \left(\frac{1}{C_{LF}} - \frac{1}{C_{ins}^{LF}}\right)^{-1} - \left(\frac{1}{C_{HF}} - \frac{1}{C_{ins}^{HF}}\right)^{-1}, \tag{7}$$

where HF and LF refer to high and low frequency. From the measured dispersion of the capacitance at a bias corresponding to the majority carrier Fermi level being at midgap ΔC_{MG}, we obtain an interface density of states at midgap of $D_s = 3\times 10^9$ states/cm^2 eV, a value consistent with that inferred from the measurement of τ_{ph} (Fig. 2).

Shown in Fig. 4 are capacitance data on a single fluorinated wafer with different metallic gate electrodes. The shift in the position of the flat band capacitance (C_{FB}) from zero bias may arise from two causes: a built-in voltage due to metal–silicon work function differences and trapped charge in the gate insulator. The quantitative contribution of each factor to shifts in the flat band voltage (V_{FB}) is difficult to ascertain since metallic and silicon work functions at interfaces may vary appreciably from tabulated values of vacuum work functions. However, the relative shift of V_{FB} from Al to Cu to Ag are quite consistent with measurements using oxide gate insulators.[19] For devices of Fig. 4 a systematic shift to negative biases of several tenths of a volt in comparison to oxide gate insulators seems indicated. We attribute this to a larger electron affinity of fluorine bonded silicon relative to oxide bonded silicon because of the more polar nature of the silicon–fluorine bond. The absence of charging effects on the photoconductive decay curves places an upper limit of 2.5×10^{10}/cm^2 on the interface charge density.

V. CONCLUSIONS

Our measurements of the surface recombination velocity of fluorine terminated silicon surfaces and C–V measurements on MIS capacitors demonstrate that these surfaces are, to an extraordinary degree, electrically inert. That is, surface electronic states with energies within the silicon band gap are almost totally absent, $\lesssim 10^{10}$/cm^2. It is possible to speculate as to reasons for the high degree of perfection attainable for fluorinated silicon surfaces. The relatively small size of the fluorine atom permits easy access to every silicon surface dangling bond. Also this easy packing of fluorine on the silicon surface eliminates any appreciable strain and distortion on the top few silicon monolayers and may explain the apparent lack of "band tailing." As a device technology, the air sensitivity of the fluorinated silicon surface is a potential drawback. However, the gate insulator we have described demonstrates that suitable device stability may be attained. The simple low temperature processing steps, the use of nonepitaxial insulators alternative to SiO_2, and the superior quality of the silicon surface attainable all suggest that a silicon interface technology based on fluorinated surfaces is a realistic possibility.

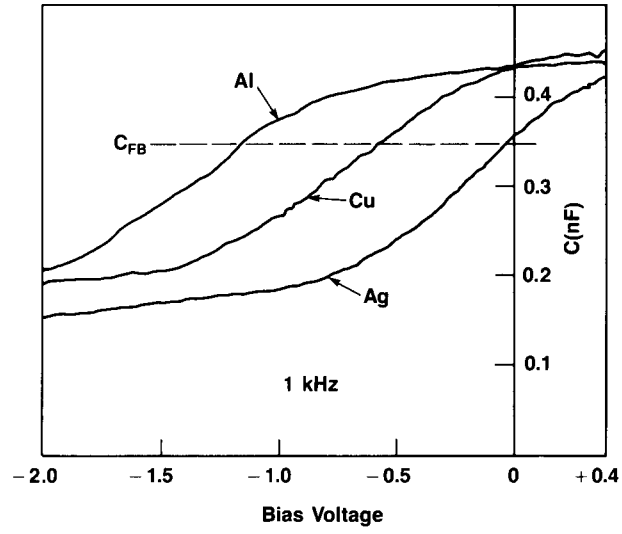

FIG. 4. Comparison of CV characteristics for different metallic gate electrodes. (Same wafer as Figs. 2 and 3).

[1] E. H. Nicollian and J. R. Brews, *MOS Physics and Technology* (Wiley, New York, 1982).
[2] J. Singh and A. Madhukar, J. Vac. Sci. Technol. **19**, 437 (1981).
[3] T. M. Buck and F. S. McKim, J. Electrochem. Soc. **105**, 709 (1958).
[4] H. Ishiwara and T. Asano, Appl. Phys. Lett. **40**, 66 (1982).

[5]J. M. Phillips, L. C. Feldman, J. M. Gibson, and M. L. McDonald, Thin Solid Films **107**, 217 (1983).
[6]T. Asano, H. Ishiwara, and N. Kaifu, Jpn. J. Appl. Phys. **22**, 1471 (1983).
[7]T. P. Smith, J.M. Phillips, W. M. Augustyniak, and P. J. Styles, Appl. Phys. Lett. **45**, 907 (1984).
[8]J. Tanguy, Thin Solid Films **13**, 33 (1972).
[9]I. Lundstrom, Phys. Scr. **18**, 424 (1978).
[10]F. R. McFeely, J. F. Morar, N. D. Shinn, G. Landgren, and F. J. Himpsel, Phys. Rev. **B 30**, 764 (1984).
[11]G. L. Miller, D. A. H. Robinson, and S. D. Ferris, Proc. Electrochem. Soc. **78-3**, 1 (1978).
[12]A. S. Grove, *Physics and Technology of Semiconductor Devices* (Wiley, New York, 1967), p. 136.
[13]Reference 1, p. 297
[14]Reference 12, p. 129
[15]Reference 12, p. 139.
[16]D. C. Northrop and O. Simpson, Proc. R. Soc. **A 234**, 124 (1956).
[17]C. Weaver, Adv. Phys. **11**, 83 (1962).
[18]Reference 1, p. 332.
[19]B. E. Deal, E. H. Snow, and C. A. Mead, J. Phys. Chem. Solids **27**, 1873 (1966).